Supplementary Materials: High-Throughput Synthesis of Pillared-Layered Magnesium Tetraphosphonate Coordination Polymers: Framework Interconversions and Proton Conductivity Studies

Rosario M.P. Colodrero, Inés R. Salcedo, Montse Bazaga-García, Eleni Barouda, Maria Papadaki, Konstantinos E. Papathanasiou, Daniel Hernández-Alonso, Jordi Rius, Miguel A.G. Aranda, Enrique R. Losilla, Pascual Olivera-Pastor, Konstantinos D. Demadis and Aurelio Cabeza

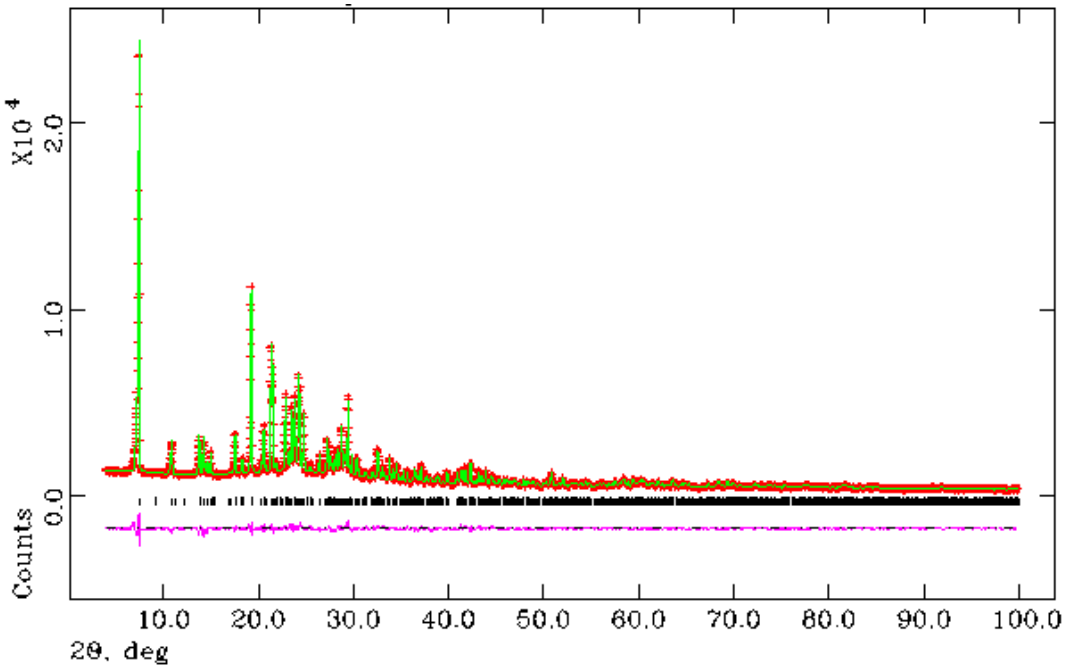

Figure S1. XRPD Rietveld plots for **Mg[(HO$_3$PCH$_2$)$_2$N(CH$_2$)$_6$N(CH$_2$PO$_3$H$_2$)$_2$]·(H$_2$O) (1)**.

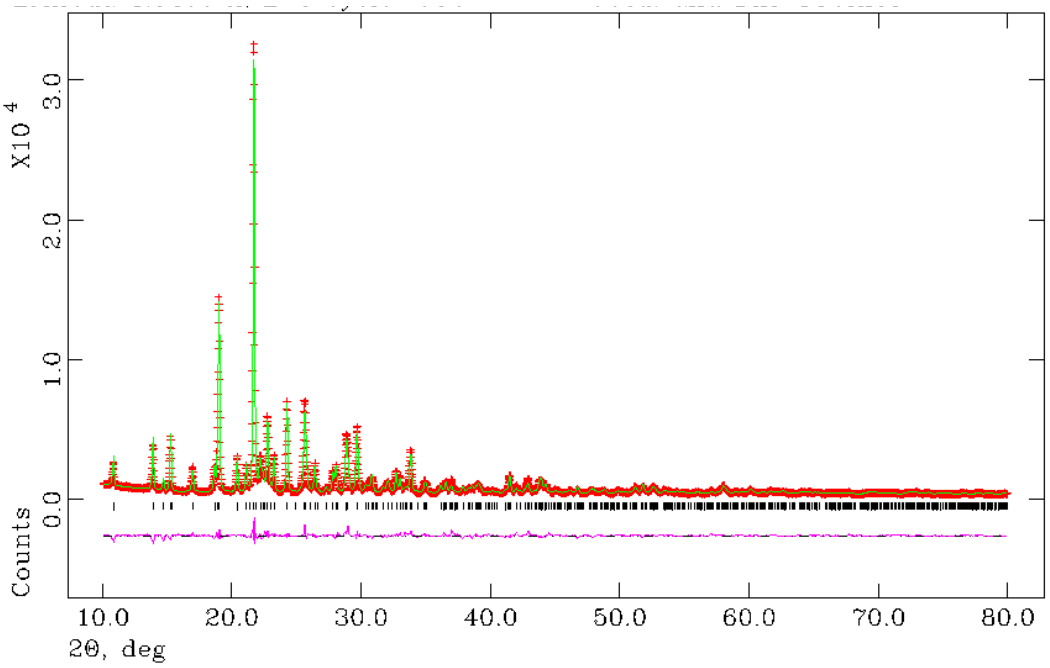

Figure S2. XRPD Rietveld plots for **Mg[(HO$_3$PCH$_2$)$_2$N(CH$_2$)$_6$N(CH$_2$PO$_3$H$_2$)$_2$] (1deh)**.

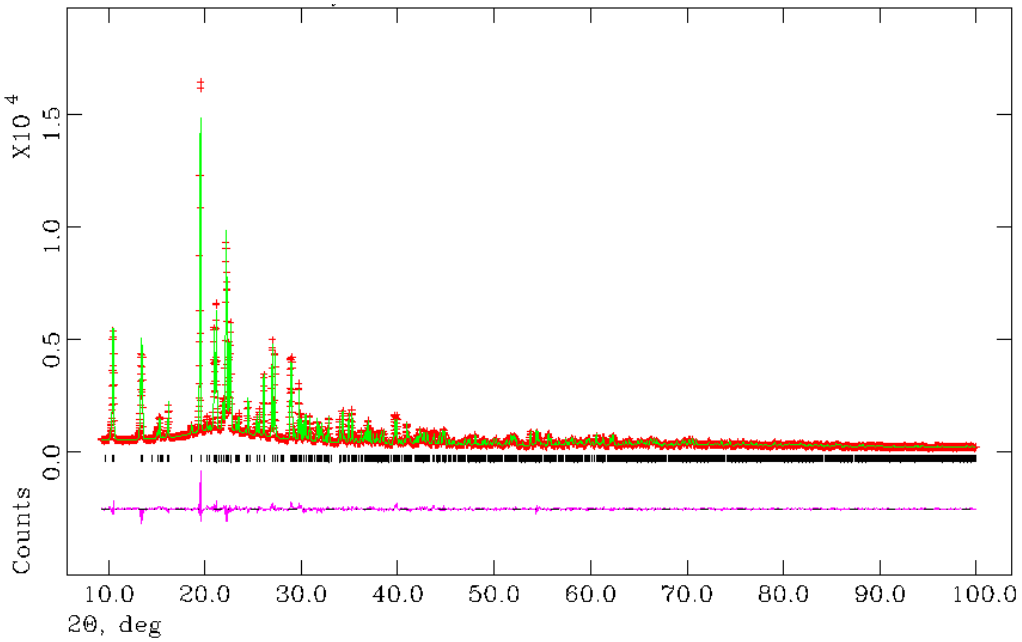

Figure S3. XRPD Rietveld plots for **Mg[(HO$_3$PCH$_2$)$_2$N(CH$_2$)$_6$N(CH$_2$PO$_3$H$_2$)$_2$] (2)**.

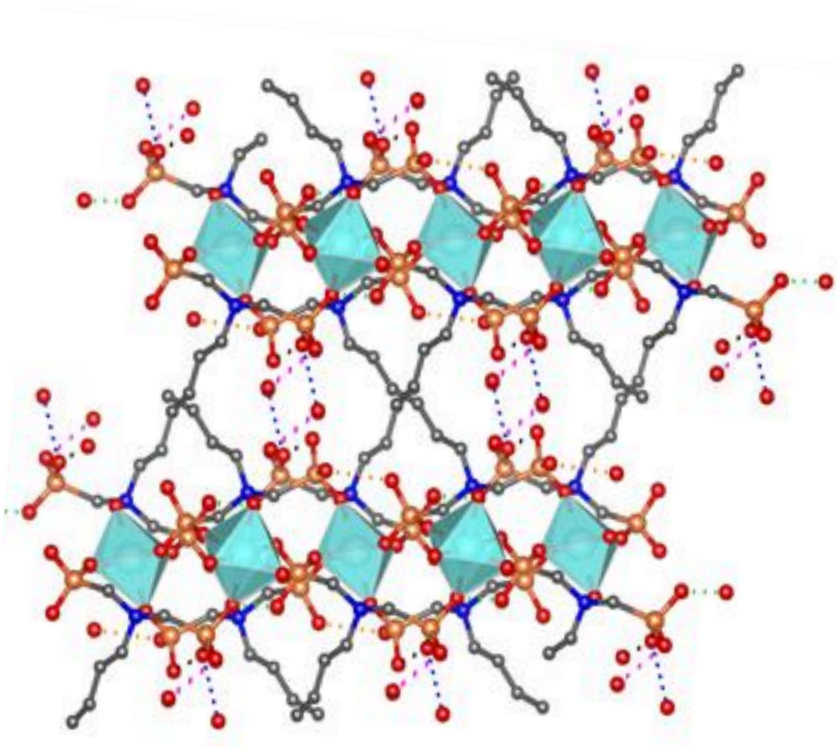

Figure S4. *b*-axis view of the H-bond interactions in **Mg[(HO$_3$PCH$_2$)$_2$N(CH$_2$)$_6$N(CH$_2$PO$_3$H$_2$)$_2$]·(H$_2$O) (1)**, O2-O6 *2.483(15)* green; O4-H$_2$O *2.586(18)* pink; O5-H$_2$O *2.605(16)* blue; O7-O10 *2.647(14)* orange and O5-O8 *2.631(13)* black dotted lines.

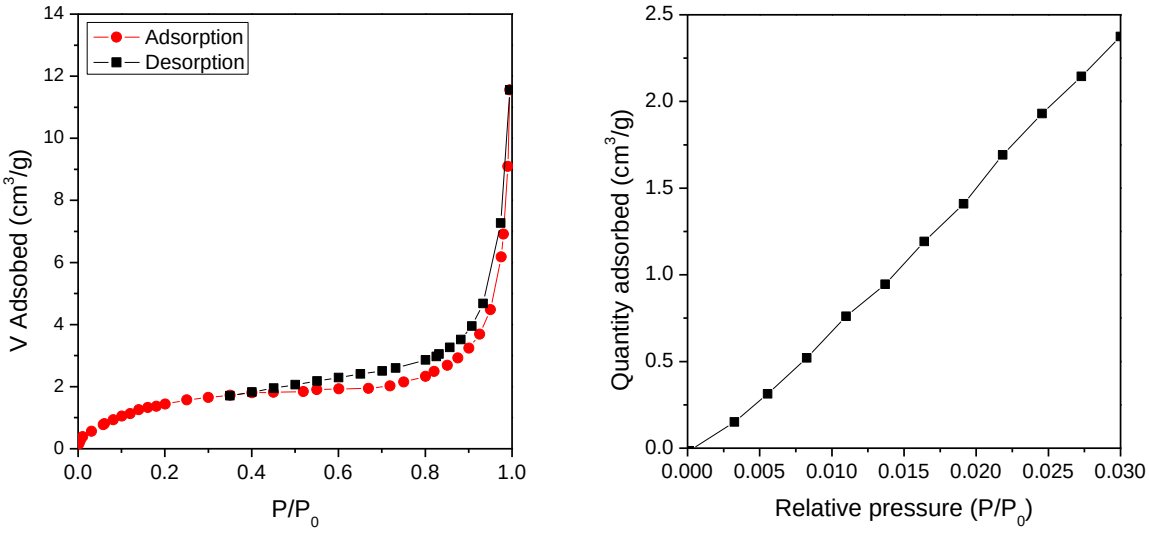

(**a**) (**b**)

Figure S5. N$_2$ (**a**) and CO$_2$ (**b**) adsorption/desorption isotherms for **Mg[(HO$_3$PCH$_2$)$_2$N(CH$_2$)$_6$N(CH$_2$PO$_3$H$_2$)$_2$]·(H$_2$O) (1)**.

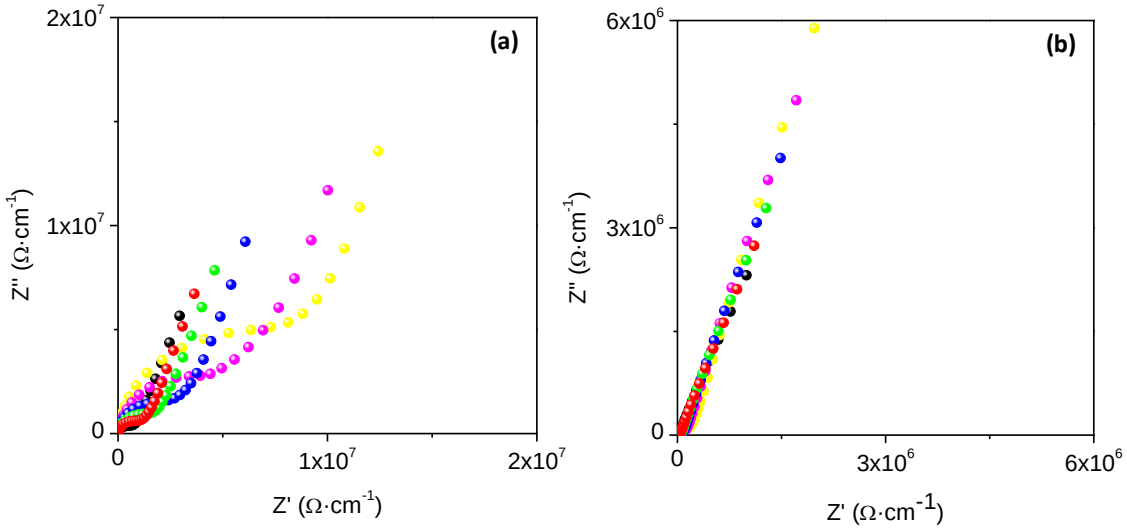

Figure S6. Nyquist plots for **Mg[(HO$_3$PCH$_2$)$_2$N(CH$_2$)$_6$N(CH$_2$PO$_3$H$_2$)$_2$]·(H$_2$O) (1)** at **(a)** 75% and **(b)** 95% RH and temperatures: 80 (black), 70 (red), 60 (green), 50 (blue), 40 (magenta) and 30 °C (yellow).

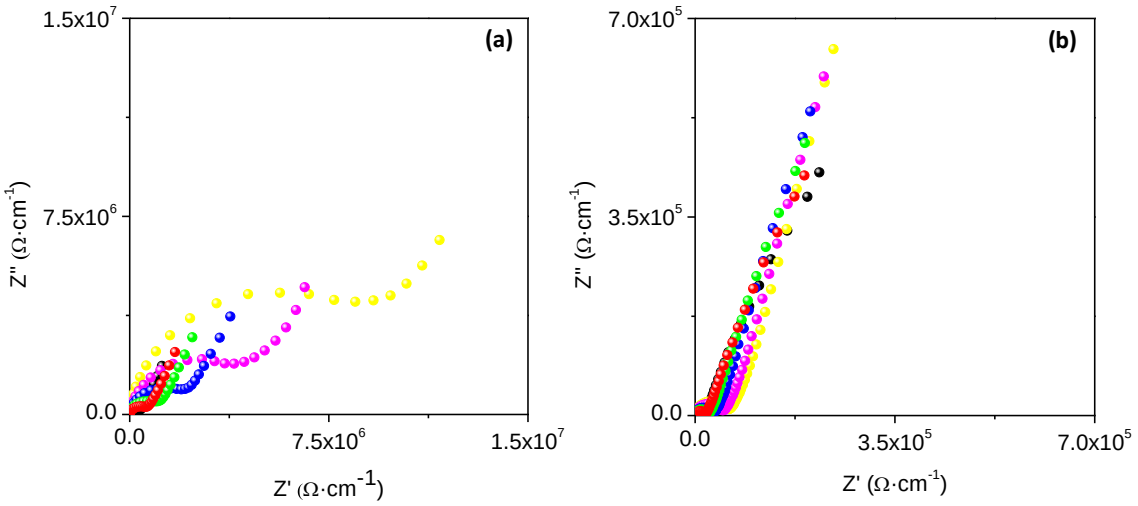

Figure S7. Nyquist plots for **Mg[(HO$_3$PCH$_2$)$_2$N(CH$_2$)$_6$N(CH$_2$PO$_3$H$_2$)$_2$] (H$_2$O) (1deh)** at **(a)** 75% and **(b)** 95% RH and temperatures: 80 (black), 70 (red), 60 (green), 50 (blue), 40 (magenta) and 30 °C (yellow).

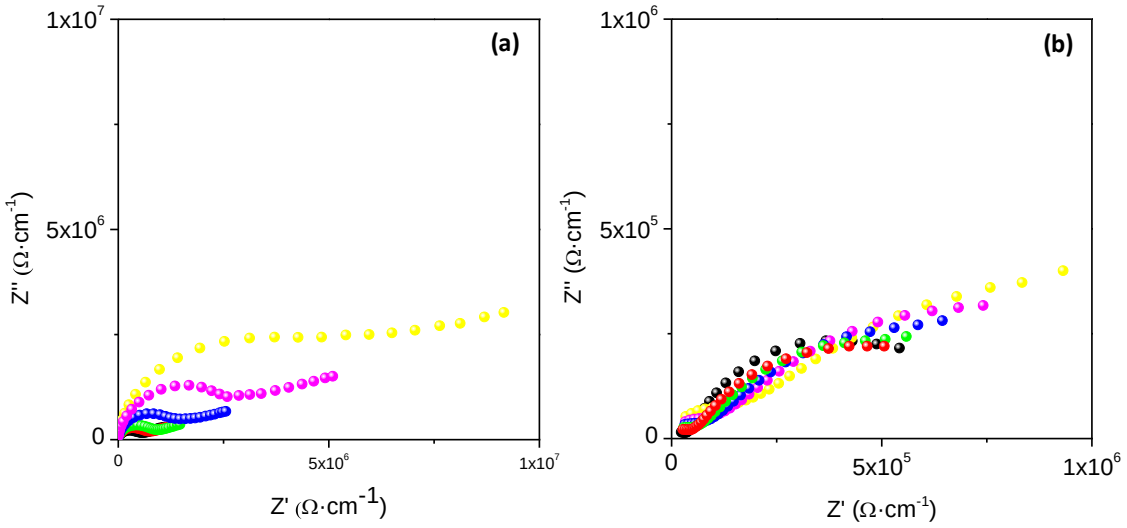

Figure S8. Nyquist plots for **Mg[(HO$_3$PCH$_2$)$_2$N(CH$_2$)$_6$N(CH$_2$PO$_3$H$_2$)$_2$] (2)** at **(a)** 75% and **(b)** 95% RH and temperatures: 80 (black), 70 (red), 60 (green), 50 (blue), 40 (magenta) and 30 °C (yellow).

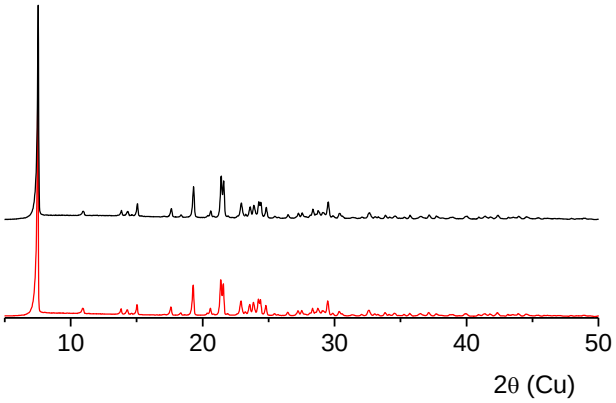

Figure S9. X-ray powder diffraction patterns for **Mg[(HO$_3$PCH$_2$)$_2$N(CH$_2$)$_6$N(CH$_2$PO$_3$H$_2$)$_2$]·(H$_2$O) (1)** as synthesized (red) and after impedance measurement (black).

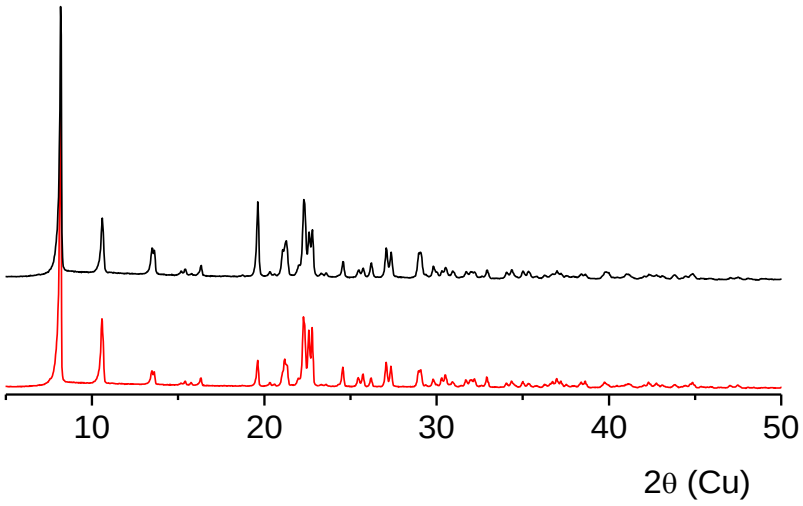

Figure S10. X-ray powder diffraction patterns for **Mg[(HO$_3$PCH$_2$)$_2$N(CH$_2$)$_6$N(CH$_2$PO$_3$H$_2$)$_2$] (2)** as synthesized (red) and after impedance measurement (black).

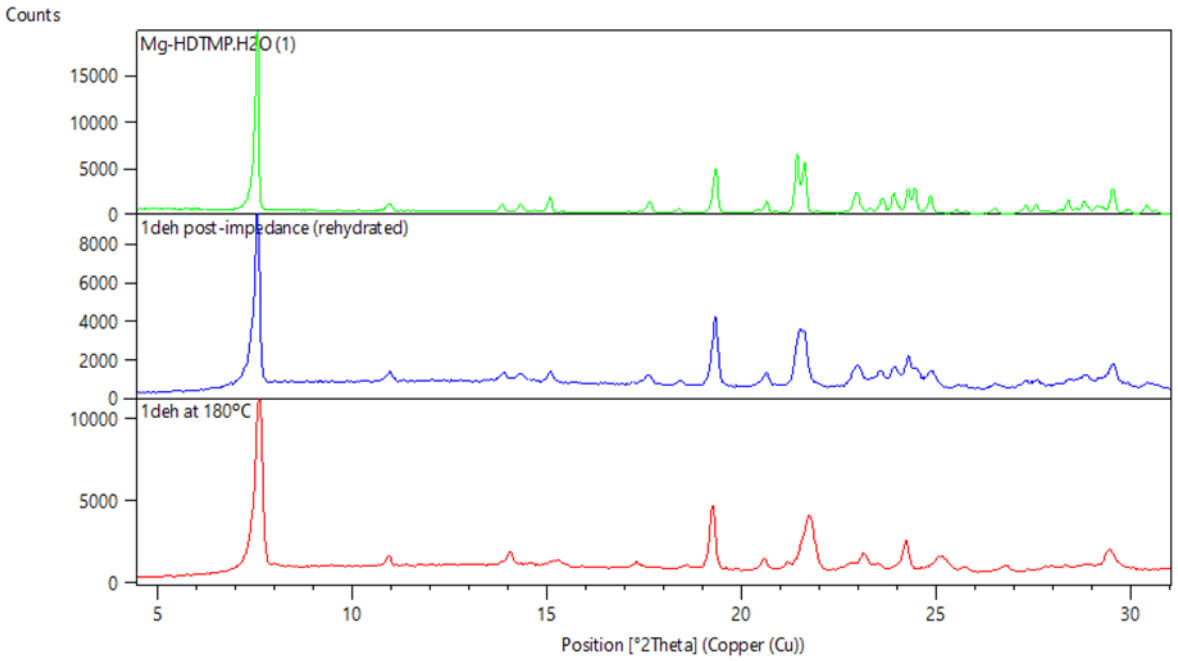

Figure S11. X-ray powder diffraction patterns for **Mg[(HO$_3$PCH$_2$)$_2$N(CH$_2$)$_6$N(CH$_2$PO$_3$H$_2$)$_2$] (1deh)** at 180 °C, after impedance measurements and **Mg[(HO$_3$PCH$_2$)$_2$N(CH$_2$)$_6$N(CH$_2$PO$_3$H$_2$)$_2$]·(H$_2$O) (1)** for comparative purposes.

Table S1. Hydrogen bond distances for **Mg[(HO$_3$PCH$_2$)$_2$N(CH$_2$)$_6$N(CH$_2$PO$_3$H$_2$)$_2$]·(H$_2$O) (1)**.

D····A	D····A (Å)	D····A	D····A (Å)
O1····O2	2.534(8)	O5····N2	3.067(13)
O1····O3	2.507(8)	O5···· H$_2$O	2.606(17)
O1····O9	2.946(12)	O6····O12	2.940(13)
O1····O11	2.823(12)	O7····O8	2.555(8)
O2····O3	2.526(8)	O7····O9	2.543(8)
O2····O6	2.483(12)	O7····O10	2.647(12)
O3····O6	2.944(12)	O7····H$_2$O	2.841(15)
O3····O12	2.883(13)	O8····O9	2.532(8)
O3····N1	2.820(12)	O9····O11	2.831(11)
O4····O5	2.536(8)	O10····O11	2.553(8)
O4····O6	2.521(8)	O10····O12	2.503(8)
O4····H$_2$O	2.585(14)	O11····O12	2.499(8)
O5····O8	2.631(12)	O11····N2	3.080(11)

Table S2. Hydrogen bond distances for **Mg[(HO$_3$PCH$_2$)$_2$N(CH$_2$)$_6$N(CH$_2$PO$_3$H$_2$)$_2$]-(1deh)**.

D····A	D····A (Å)	D····A	D····A (Å)
O1····O2	2.430(10)	O4····O5	2.946(13)
O1····O3	2.597(9)	O4····O5	2.433(9)
O1····O4	2.983(10)	O4····O6	2.377(9)
O1····O5	2.990(11)	O4····N	3.146(14)
O2····O3	2.512(10)	O5····O6	2.525(9)
O3····O6	2.950(11)	O5····N	2.840(14)

Table S3. Hydrogen bond distances for **Mg[(HO$_3$PCH$_2$)$_2$N(CH$_2$)$_6$N(CH$_2$PO$_3$H$_2$)$_2$] (2)**.

D····A	D····A (Å)	D····A	D····A (Å)
O1····O2	2.560(7)	O5····O11	2.454(10)
O1····O3	2.530(7)	O6····O7	2.830(11)
O1····O7	2.862(11)	O6····N2	2.791(12)
O1····O12	3.044(11)	O7····O8	2.570(7)
O2····O3	2.491(7)	O7····O9	2.483(7)
O2····O6	2.896(13)	O7····N2	3.059(13)
O2····O7	2.962(10)	O8····O9	2.533(8)
O2····N2	3.011(12)	O9····N1	3.052(12)
O3····O9	2.901(10)	O9····O10	2.938(9)
O3····O10	2.909(10)	O10····N1	2.736(12)
O3····O12	2.862(12)	O10····O11	2.540(7)
O4····O5	2.559(7)	O10····O12	2.531(7)
O4····O6	2.556(7)	O11····O12	2.548(7)
O5····O6	2.506(7)		